HHS Public Access

Author manuscript

Shock. Author manuscript; available in PMC 2017 June 01.

Published in final edited form as:

Shock. 2016 June ; 45(6): 677–685. doi:10.1097/SHK.0000000000000550.

Enhanced glucose transport, but not phosphorylation capacity, ameliorates lipopolysaccharide-induced impairments in insulin stimulated-muscle glucose uptake

Yolanda F. Otero[#,†], **Kimberly X. Mulligan**[#,†], **Tammy M. Barnes**[#,¥], **Eric A. Ford**[#,‡], **Carlo M. Malabanan**[#], **Haihong Zong**[*], **Jeffrey E. Pessin**[*], **David H. Wasserman**[#], and **Owen P.M Guinness**[#,c]

[#]Department of Molecular Physiology and Biophysics, Vanderbilt University School of Medicine, Nashville, TN 37232-0615 USA

[‡]College of Medicine, University of Tennessee Health Science Center, Memphis, TN 38163 USA

[¥]Department of Internal Medicine, University of Michigan, Ann Arbor, MI 48109 USA

[*]Department of Medicine and Molecular Pharmacology, Albert Einstein College of Medicine, Bronx, NY 10461 USA

Abstract

Lipopolysaccharide (LPS) is known to impair insulin stimulated muscle glucose uptake. We determined if increased glucose transport (GLUT4) or phosphorylation capacity (hexokinase II; HKII) could overcome the impairment in muscle glucose uptake (MGU). We utilized mice that over-expressed GLUT4 ($GLUT4^{Tg}$) or HKII (HK^{Tg}) in skeletal muscle. Studies were performed in conscious, chronically catheterized (carotid artery and jugular vein) mice. Mice received an intravenous bolus of either LPS (10μg/g body weight) or vehicle (VEH). After 5 h, a hyperinsulinemic-euglycemic clamp was performed. As MGU is also dependent on cardiovascular function that is negatively affected by LPS, cardiac function was assessed using echocardiography. LPS decreased whole body glucose disposal and MGU in WT and HK^{Tg} mice. In contrast, the decrease was attenuated in $GLUT4^{Tg}$ mice. While membrane-associated GLUT4 was increased in VEH-treated $GLUT4^{Tg}$ mice, LPS impaired membrane-associated GLUT4in $GLUT4^{Tg}$ mice to the same level as LPS-treated WT mice. This suggested that overexpression of GLUT4 had further benefits beyond preserving transport activity. In fact, GLUT4 overexpression attenuated the LPS-induced decrease in cardiac function. The maintenance of MGU in $GLUT4^{Tg}$ mice following LPS was accompanied by sustained anaerobic glycolytic flux as suggested by increased muscle *Pdk4* expression, and elevated lactate availability. Thus, enhanced glucose transport, but not phosphorylation capacity, ameliorates LPS-induced impairments in MGU. This benefit is mediated by long-term adaptations to the overexpression of GLUT4 that sustain muscle anaerobic glycolytic flux and cardiac function in response to LPS.

[c]Corresponding author: Owen P M Guinness, Ph D, 702 Light Hall, Dept. Molecular Physiology and Biophysics, Vanderbilt University, Nashville, TN 37232-0615, Phone: (615) 343-4473, Fax: (615) 322-1462, owen.mcguinness@vanderbilt.edu.
[†]YF Otero and KX Mulligan have contributed equally

Conflict of interest: none

Disclosures: The authors have no conflicts of interest related to this article.

Keywords

inflammation; insulin resistance; cardiac output; endotoxin

Introduction

Hospitalized individuals especially in those with an accompanying infection are prone to hyperglycemia. While there was initial enthusiasm that severe glucose control in the hospitalized setting would improve outcomes in the critically ill patient, subsequent data have observed negative outcomes (1, 2). The main approach to normalize glycemia is to administer exogenous insulin. Unfortunately, this increases the risk of hypoglycemia (3, 4). Thus, a better understanding of the factors that contribute to infection-induced insulin resistance is needed to better control hyperglycemia in the hospitalized setting

Infection and lipopolysaccharide (LPS), a potent proinflammatory factor of Gram-negative bacteria, impair muscle glucose uptake (MGU) (5-7). Skeletal muscle represents the bulk of insulin-sensitive tissue in the body, and is a major site of glucose disposal. The regulation of glucose uptake in the skeletal muscle is distributed over three-steps: 1) vascular delivery of glucose to the tissue and its subsequent diffusion into the interstitium, 2) facilitated transport into the intracellular space by glucose transporters (GLUT), and 3) irreversible phosphorylation of glucose to glucose-6-phosphate (G6P) by hexokinase (HK) (8). Each step is regulated by a number of factors which can be modulated by insulin as well as impaired by LPS (9, 10).

It is unknown whether targeting one or more of those steps would improve MGU in response to LPS. Several studies in other settings where insulin action in muscle is altered (obesity and exercise) have increased or decreased the amounts of GLUT4 and HK to assess the importance of transport and glucose phosphorylation in determining insulin action (11-13). GLUT4 is the main glucose transporter responsible for insulin-stimulated glucose uptake and it is mainly expressed in skeletal muscle, heart and adipose tissue, and translocates to the plasma membrane upon insulin stimulation. In the current study we used transgenic mouse models that overexpress HKII or GLUT4 in skeletal muscle to determine if lowering these barriers to glucose uptake will improve insulin-stimulated MGU in the presence of LPS. We observed that improving glucose transport (GLUT4 overexpression) but not phosphorylation capacity (HKII overexpression) improved basal and insulin-stimulated MGU. Surprisingly, GLUT4 overexpression did not attenuate the LPS-induced decrease in membrane-associated GLUT4. It did, however, attenuate the LPS-induced decrease in cardiac function, and upregulate anaerobic glycolysis, which may have contributed to the improvement in MGU.

Methods

Animal Care and Husbandry

Mice on a C57Bl/6J background selectively overexpressing HKII ($HKII^{Tg}$) in skeletal muscle using a transgene containing the human HKII cDNA driven by the rat muscle

creatine kinase promoter, and mice transgenic for the *hGLUT4-11.5* construct ($GLUT4^{Tg}$) were studied (14, 15). At three weeks of age, mice were separated by gender and maintained in micro-isolator cages on a 12-h light/dark cycle with free access to food and water. All experiments were performed on male mice that were $HKII^{Tg}$, $GLUT4^{Tg}$, or wild-type (WT) littermates at ∼3 months of age. All procedures performed were approved by the Vanderbilt University Institutional Animal Care and Use Committee.

Surgical Procedures

Chronic catheters were surgically implanted as previously described (16). Briefly, mice were anesthetized with Isoflurane. The left carotid artery and right jugular vein were catheterized for sampling and infusions, respectively. The free ends of the catheters were tunneled under the skin to the back of the neck where the loose ends of the catheters were attached via stainless steel connectors to tubing made of Micro-Renathane, which were exteriorized and sealed with stainless steel plugs. Animals were individually housed after surgery, and body weight was recorded daily.

In Vivo Metabolic Experiments

All metabolic experiments were performed following a ∼5-day postoperative recovery period as previously described (5). For metabolic studies, conscious, unrestrained catheterized mice were placed in ∼1-L plastic container lined with bedding and fasted at 7:00 am (t= -300 min). The animals were immediately connected to a Dual Channel Stainless Steel Swivel (Instech Laboratories, Plymouth Meeting, PA) to allow simultaneous jugular vein infusion and sampling of arterial blood. Mice were not handled on the day of study and allowed to move freely to eliminate stress. At t= -240 min, the mice received a bolus of vehicle (VEH; saline) or *E. coli* endotoxin (*E. coli* 011:B4; Lot#129K4025, Sigma-Aldrich, St. Louis, MO) at 10 μg/g BW into the jugular vein catheter. A 5 μCi bolus of 3-[^{3}H]-D-glucose was given into the jugular vein at t=-120 min followed by a constant infusion at a rate of 0.05 μCi/min. Following a 2 h equilibrium period (t=0 min), a baseline arterial blood sample was drawn for measurement of blood glucose, 3-[^{3}H]-D-glucose, hematocrit, plasma insulin, and plasma cytokine levels. Red blood cells from a donor mouse on a C57Bl/6j background washed with 0.9% heparinized saline were infused at a rate of 4 μl/min for the duration of the study to minimize falls in the hematocrit.

Plasma glucose levels and tissue glucose uptake were assessed in six groups [WT VEH (n=7), WT LPS (n=8), $HKII^{Tg}$ VEH (n=8), $HKII^{Tg}$ LPS (n=8), $GLUT4^{Tg}$ VEH (n=8), $GLUT4^{Tg}$ LPS (n=7)] 6 hours after administration of LPS or VEH befor initiation of the clamp (i.e. pre-clamp). A hyperinsulinemic-euglycemic (120 mg/dl) clamp was used to assess insulin action in six groups [WT VEH (n=8), WT LPS (n=8), $HKII^{Tg}$ VEH (n=9), $HKII^{Tg}$ LPS (n=9), $GLUT4^{Tg}$ VEH (n=13), $GLUT4^{Tg}$ LPS (n=10)]. As we previously observed that LPS impairs insulin clearance, a lower dose of insulin (2 *vs.* 4 $mU \cdot kg^{-1} \cdot min^{-1}$) was used in LPS-treated animals to match arterial insulin concentration between groups (5). Arterial blood samples were taken every ten minutes to determine blood glucose levels. At t= 70, 80, 90 and 100 min, blood samples were taken to determine 3-[^{3}H]-D-glucose. At t= 100 min, a 13 μCi bolus of 2-deoxy [^{14}C] glucose ([2-^{14}C]DG) was administered into the jugular vein catheter to assess tissue glucose uptake. At t= 102, 105, 110, 115, and 125 min,

arterial blood was sampled to determine blood glucose, plasma 3-[^{3}H]-D-glucose and [2-^{14}C]DG. At t= 125 min, a final arterial blood sample was taken to assess all hormones and plasma [2-^{14}C]DG. The mice were then anesthetized. The *soleus, gastrocnemius, superficial white vastus lateralis* (SVL), gonadal adipose tissue (AT), liver, heart, and brain were excised, immediately frozen in liquid nitrogen, and stored at -70°C until future tissue analysis.

Plasma and muscle sample analysis

Immunoreactive insulin was assayed using a Linco Rat Radioimmunoassay kit (Linco Research, Inc., St. Charles, MO) and a double antibody method. Plasma FFA levels were measured enzymatically using a commercially available kit (NEFA C; Wako Chemicals USA). Plasma lactate levels were determined in a 96-well plate using a modification of the method of Lloyd *et al.* (17). To measure 3-[^{3}H]-D-glucose and [2-^{14}C]DG in the plasma, samples were deproteinized with barium hydroxide and zinc sulfate, dried, and radioactivity was determined using liquid scintillation counting (TriCarb Liquid Scintillation Analyzer; PerkinElmer Life and Analytical Sciences, Downers Grove, IL). Excised *soleus*, *gastrocnemius*, superficial *vastus lateralis* (SVL), gonadal adipose tissue (AT), heart, and brain were deproteinized with perchloric acid and subsequently neutralized to a pH of ∼7.5. A portion of the sample was counted ([2-^{14}C]DG and [2-^{14}C]DG-G-phosphate ([2-^{14}C]DGP), while a portion was treated with $Ba(OH)_2$ and $ZNSO_4$, and the supernatant was counted ([2-^{14}C]DG). Both [2-^{14}C]DG and [2-^{14}C]DG-G-phosphate ([2-^{14}C]DGP) radioactivity levels were determined using liquid scintillation counting.

Calculations

Glucose flux rates were assessed using non-steady state equations assuming a volume of distribution (130 ml/kg). Tissue-specific clearance (K_g) of [2-^{14}C]DG, and glucose uptake (R_g) were calculated as previously described (5):

$$K_g = [2-{}^{14}\mathrm{C}]\mathrm{DGP}_{\mathrm{tissue}} / \mathrm{AUC}[2-{}^{14}\mathrm{C}]\mathrm{DG}_{\mathrm{plasma}}$$

$$R_g = (K_g)([\mathrm{glucose}]_{\mathrm{plasma}})$$

where [2-^{14}C]DGP_{tissue} is the [2-^{14}C]DGP radioactivity (dpm/g) in the tissue, AUC [2-^{14}C]DG_{plasma} is the area under the plasma [2-^{14}C]DG disappearance curve (dpm/mL/min), and $[glucose]_{plasma}$ is the average blood glucose (μg/μl) during the experimental period.

Echocardiography

Transthoracic echocardiography was performed using a system (Sonos 5500, Agilent, Andover, MA) with a 15-MHz high frequency linear transducer at a frame rate of 100 frames/sec. All images were acquired at a depth setting of 20 mm. Images were acquired at two time points: t= 0 min, which represents the time immediately prior to an injection of VEH or LPS and at t= 360 min. The mouse was picked up at the nape of its neck, and an

ultrasound-coupling gel was applied to the precordium with the ultrasound probe. Two-dimensional targeted M-mode echocardiographic images were obtained at the level of the papillary muscles from the parasternal short-axis views and recorded at a speed of 150cm/s (maximal temporal resolution) for measurements of heart rate. All other measurements were made on-screen using the digitally recorded signals. Stroke volume and cardiac output were calculated using the equations shown below:

$$\text{End Diastolic Volume}\,(\mu\text{L}) = (7/(2.4 + \text{LVIDd}))^{*}(\text{LVIDd}^{3})$$

$$\text{End Systolic Volume}\,(\mu\text{L}) = (7/(2.4 + \text{LVIDs}))^{*}(\text{LVIDs}^{3})$$

$$\text{Stroke Volume}(\mu\text{L}) = \text{End Diastolic Volume} - \text{End Systolic Volume}$$

$$\text{Cardiac Output}(\text{mL} \cdot \text{min}^{-1}) = (\text{Stroke Volume} * \text{Heart Rate})/100$$

where LVIDd and LVIDs are left ventricular internal dimensions during diastole and systole, respectively.

Real-time Quantitative PCR

Heart tissues were homogenized in TRIzol (Ambion RNA, Carlsbad, CA), and mRNA was extracted. cDNA was obtained using a cDNA Reverse Transcription kit (Applied Biosystems, Lot# 66105, Foster City, CA) and stored at -20°C. PCR amplification via ABI system and TaqMan probes (for *Pdk4* and *Nos2*) allowed mRNA quantification using the ΔΔCt method. Gene expression was normalized using *Gapdh* as a housekeeping gene.

Glucose-6-phosphate assay

Heart and muscle were homogenized in perchloric acid, and supernatant was neutralized with KOH (1M). Samples and standards were incubated in a buffer containing ATP, NADP and glucose-6-phosphate dehydrogenase. NADPH fluorescence was measured.

Immunofluorescence microscopy

Tissues isolated from mice that underwent a hyperinsulinemic-euglycemic clamp were embedded in optimal cutting temperature compound. The frozen tissue cross-sections (10 μM) were blocked with 3% BSA in PBS for 60 min at room temperature. Primary antibodies were used at the following dilutions: GLUT4 polyclonal antibody (1:1000) was obtained from East Acres Biologicals Inc., and α-dystroglycan (α-DG) monoclonal antibody (1:50) was a kind gift from Dr. Kevin Campbell (The University of Iowa, Iowa City, IA), and used as previously described (18). Fluorescently conjugated secondary antibodies (1:100, Jackson ImmunoResearch Laboratories) were added to the sections for 30 min at room temperature. After extensive washing with PBS, the slides were mounted with Vectashield Mounting

Medium (Vector Laboratories). The slides were visualized by confocal fluorescent microscopy (model LSM510; Carl Zeiss MicroImaging, Inc.). Quantification of cell surface immunofluorescence was performed using NIH Image software. Briefly, individual muscle fibers were delineated by α-DG labeling and were circumscribed to obtain the total GLUT4 fluorescent intensity. The intracellular GLUT4 fluorescent intensity of the same fiber was determined by circumscribing approximately 1μm below the α-DG labeled surface. The difference between the total and intracellular signals was defined as the cell surface GLUT4. The cell surface GLUT4 intensity normalized for the intracellular GLUT4 intensity was plotted as the relative cell surface GLUT4.

Data Analysis

Data are presented as the mean ± SEM. Differences between groups were compared by two-way ANOVA and by student's t-test when appropriate. The significance level was set at $p < 0.05$.

Results

GLUT4 but not HKII Overexpression Inhibits the LPS-induced Decrease in Baseline Muscle Glucose Uptake

It has previously been shown that the GLUT4 transgene increases GLUT4 protein content 2- to 4-fold in skeletal muscle of C57BL/6 mice (14). In the presence of a saline infusion, $Glut4^{Tg}$ mice had the expected lower baseline (i.e. without exogenous insulin stimulation) insulin and glucose levels 6 hours after VEH treatment compared to their WT counterparts. While LPS led to a significant decrease in insulin levels in WT mice, the insulin levels observed in $Glut4^{Tg}$ mice treated with LPS during saline infusion failed to decrease further relative to VEH controls (Figure 1). This was also reflected in the fasting glucose concentrations. WT mice that received VEH had higher baseline glucose concentrations compared to WT mice that received LPS as well as $Glut4^{Tg}$ mice that received either VEH or LPS. Tracer determined glucose turnover rate was increased in $Glut4^{Tg}$ compared to WT mice treated with VEH (13.2±2.0 vs. 16.4±1.3 $mg \cdot kg^{-1} \cdot min^{-1}$; WT vs. $Glut4^{Tg}$), but it decreased to similar levels in the presence of LPS (9.8±3.1 vs. 11.6±1.3 $mg \cdot kg^{-1} \cdot min^{-1}$). LPS decreased baseline muscle glucose uptake in WT mice. However, $Glut4^{Tg}$ mice were protected from the LPS-induced decrease in baseline muscle glucose uptake (Figure 2A. and 2B).

In contrast to GLUT4 overexpression, HKII overexpression did not prevent the LPS-induced decrease in basal muscle glucose uptake. The HKII transgene is overexpressed 3-, 5-, and 7-fold in the *soleus, gastrocnemius*, and SVL, respectively (15). The basal glucose concentrations were similar between WT and HKII with VEH and LPS treatment (Figure 1), and there was neither significant improvement in baseline tissue glucose uptake nor LPS-induced tissue glucose uptake (Figure 2C and 2D). There were no significant differences in insulin levels between $HKII^{Tg}$ and WT mice with VEH treatment. LPS decreased baseline insulin to a similar extent as WT (Figure 1).

GLUT4 but not HKII Overexpression Inhibits LPS-induced Decreases in Insulin-Stimulated Muscle Glucose Uptake

A hyperinsulinemic-euglycemic clamp was used to assess insulin action in $GLUT4^{Tg}$, $HKII^{Tg}$ and WT mice. Insulin levels increased during the clamp and were matched between both groups with VEH and LPS treatment, and glucose concentrations were maintained at ∼120 mg/dl (Figure 3 and 4A). Both $GLUT4^{Tg}$ and WT mice had similar glucose infusion rate (GIR; $mg \cdot kg^{-1} \cdot min^{-1}$) with VEH treatment (59.5 ± 0.2 vs. 54.2± 0.5, respectively; Figure 4B). However, in $GLUT4^{Tg}$ mice, LPS did not impair the GIR to the same extent as WT mice (decreased by 23% vs. 35%; 45.6 ± 0.2 vs. 35.4 ± 0.6; Figure 4B). LPS decreased glucose uptake in the *gastrocnemius* and SVL of WT mice compared to VEH treatment. In contrast, in $GLUT4^{Tg}$ mice, LPS failed to suppress muscle glucose uptake (Figure 4C & 4D).

On the other hand, under hyperinsulinemic-euglycemic clamp conditions, $HKII^{Tg}$ and WT mice had a similar GIR with VEH treatment, and GIR decreased similarly with LPS treatment (54.6 ± 0.5 vs. 54.2± 0.5; 35.6 ± 0.4 vs. 35.4 ± 0.6, respectively; Figure 5B). This translated into a significant decrease in glucose uptake in the *gastrocnemius*, SVL, and heart in both $HKII^{Tg}$ and WT mice with LPS treatment (Figure 5C, 5D).

GLUT4 Overexpression Increases Arterial Lactate Levels

$GLUT4^{Tg}$ mice had significantly higher arterial lactate levels following VEH treatment compared to WT mice (Figure 6). LPS modestly increased lactate concentration in WT mice. LPS did not further increase the already elevated lactate in $GLUT4^{Tg}$ mice. However, during the clamp, lactate concentration markedly increased in $GLUT4^{Tg}$ mice. In HK^{Tg} lactate was similar to that seen in WT mice. As overexpression of HKII had no phenotype in terms of alterations in MGU, GIR, or plasma lactate, we focused on further characterizing the phenotype of the GLUT4 overexpressing mice.

GLUT4 Overexpression Increases Plasma Non-Esterified Free Fatty Acids (NEFAs)

Increased NEFA's can impair MGU. We determined if the improvement in insulin-stimulated MGU in response to LPS observed with overexpression of GLUT4 could be due to improved suppression of plasma NEFAs during the hyperinsulinemic-euglycemic clamp. In fact, this was not the case. During the basal period, $GLUT4^{Tg}$ tended to have higher plasma NEFA levels with VEH treatment (Table 1). However, during the clamp, plasma NEFAs did not decrease in $GLUT4^{Tg}$ to the same extent as observed in WT mice. With LPS treatment, plasma NEFA levels were increased ∼2-fold during the pre-clamp period (i.e. prior to initiation of the clamp but 6 hr after treatment with LPS) and decreased during the clamp to a similar extent in $GLUT4^{Tg}$ compared to WT mice.

GLUT4 Overexpression does not prevent LPS-induced decrease in Plasma Membrane-Associated GLUT4

GLUT4 association with the plasma membrane in gastrocnemius muscle of mice that underwent a hyperinsulinemic-euglycemic clamp was examined by immunohistochemistry. The muscle fiber cell surface distribution of GLUT4 was co-localized with the sarcolemma marker protein α-DG. With vehicle treatment, there was a relative increase in cell surface-

associated GLUT4 in transgenic compared to WT mice. LPS decreased cell surface GLUT4 to similar levels in both WT and transgenic mice (Figure 7). As an increase in transport activity can be offset by a corresponding defect in downstream glycolysis, we examined whether overexpression of GLUT4 would lead to a corresponding increase in glucose 6 phosphate in the presence of inflammatory stress. In fact, glucose-6-phosphate content (μmol/mg) in the SVL (3.2±0.1 vs 3.7±0.1; WT vs. $GLUT4^{Tg}$) and heart (5.9±0.8 WT vs. 6.6±1.0 $GLUT4^{Tg}$) in LPS treated animals, were unaltered by overexpression of GLUT4. This suggests that events occurring outside the myocyte contributed to the protection afforded by overexpression of GLUT4.

GLUT4 Overexpression Improves Cardiac Function and increases Pdk4 expression

The effect of LPS treatment on cardiovascular parameters in $GLUT4^{Tg}$ compared to WT mice was examined. Stroke volume, heart rate and cardiac output decreased in both groups treated with LPS compared to their vehicle-treated counterparts (Table 2). However, while LPS-treatment led to a ∼50% decrease in stroke volume and cardiac output in WT animals, the fall was attenuated in $GLUT4^{Tg}$ mice.

To determine if the cardiac protection for LPS with GLUT4 overexpression was due to altered cardiac glucose oxidation or attenuated cardiac inflammation, we assessed cardiac gene expression of *Pdk4* and *Nos2* (i.e. iNOS). Cardiac muscle *Pdk4* expression was increased in $GLUT4^{Tg}$ following VEH treatment, which is indicative of a decrease in glucose oxidation (Figure 8). LPS treatment markedly increased *Pdk4* expression in WT but did not further elevate expression in $GLUT4^{Tg}$. Cardiac muscle *Nos2* expression was decreased in $GLUT4^{Tg}$ following VEH (Figure 8). LPS increased *Nos2* expression in WT and $GLUT4^{Tg}$ to a similar level, suggesting cardiac inflammation was augmented to a similar extent.

Discussion

LPS induces marked insulin resistance. We enhanced the glucose transport or phosphorylation capacity of the muscle to determine if either could overcome the LPS-induced impairment in insulin action *in vivo*. We demonstrate that increasing the ability to transport glucose, but not phosphorylate glucose, prevents the LPS-induced impairment in MGU *in vivo*. Surprisingly, GLUT4 overexpression did not preserve membrane associated GLUT4 at the sarcolemmal membrane in the presence of LPS. It did, however, attenuate the LPS-induced impairment in cardiac output and induced adaptations that sustained anaerobic glycolysis. Our previous findings suggested that alterations in muscle glucose delivery play a critical role in insulin resistance resulting from LPS (5, 19). These results suggest that the protective effect of GLUT4 overexpression is not due to maintenance of transport capacity but in part due to the maintenance of cardiac function in response to LPS.

Overexpression of GLUT4 but not HKII attenuated the LPS-induced decrease in baseline MGU. In $GLUT4^{Tg}$ mice, MGU was not altered in the basal state of VEH treated animals. However, in contrast to WT and $HKII^{Tg}$, $GLUT4^{Tg}$ mice were protected from the LPS-induced decrease in baseline muscle glucose uptake. Some studies suggested GLUT4 overexpression augmented baseline MGU, implying that glucose transport is the primary site

of resistance in the basal state (20, 21). Consistent with our prior work we did not see an increase in MGU in response to saline infusion (i.e. in the absence of exogenous insulin stimulation) with GLUT4 overexpression (21). It is possible that the lower glucose concentrations in the present study may have limited our ability to detect an increase in basal MGU. One possible explanation as to how overexpression of GLUT4 sustained MGU in the presence of LPS is that chronic overexpression of GLUT4 augmented muscle glycolytic capacity. As has been previously reported, plasma lactate was in fact increased in GLUT4^{Tg} mice with VEH, and this was not observed in HKII^{Tg} mice (22). Thus, as MGU was normal, a greater fraction of the basal MGU was not oxidized but diverted to anaerobic glycolysis (i.e. lactate release); this has been observed *ex vivo* in muscle from GLUT4^{Tg} mice (23). The corresponding elevation of NEFA may have helped to further limit glucose oxidation and favor lactate release. The increase in plasma lactate may also serve to maintain the increase in basal endogenous glucose production in GLUT4^{Tg} mice with VEH treatment (24). However, as will be discussed later, accompanying improvements in the cardiovascular response to LPS in GLUT4^{Tg} would also contribute to the maintenance of MGU in response to LPS.

Overexpression of GLUT4 but not HKII also protected animals from the LPS-induced decrease in insulin action. During the hyperinsulinemic-euglycemic clamp, WT, HKII^{Tg}, and GLUT4^{Tg} mice had similar glucose infusion rates and MGU following VEH treatment. This is consistent with our prior studies demonstrating that increased GLUT4 does not augment insulin-stimulated MGU in unstressed wild type mice *in vivo* (21). However, GLUT4^{Tg} mice but not HKII^{Tg} mice were resistant to the LPS-induced decrease in whole body glucose infusion rate as well as MGU. These results indicate that strategies that augment glucose transport capacity can overcome barriers to insulin-stimulated glucose uptake induced by LPS. On the other hand, overexpression of GLUT4 could not prevent the LPS-induced decrease in membrane-associated GLUT4. Thus, in GLUT4^{Tg} mice, the maintenance of MGU in response to LPS may be secondary to adaptations to the overexpression of GLUT4 that can serve a protective role from other effects limiting MGU during inflammation. As HKII overexpression did not modify the response to LPS, we focused on the mechanism for the improvement in glucose disposal in the GLUT4^{Tg} mice.

Greater suppression of NEFA availability could not explain the improvement in MGU with GLUT4 overexpression in response to LPS. The transgenic mouse model used for these studies increased GLUT4 protein not only in muscle but also in adipose tissue (14). Plasma NEFA levels in the basal state were increased in GLUT4^{Tg} mice. In response to an increase in insulin, NEFA decreased in all groups. However, in GLUT4^{Tg} mice, NEFA remained elevated relative to WT animals. Increased basal NEFA levels in GLUT4^{Tg} mice could be due to an increase in lipolysis and/or a decrease in re-esterification (25, 26). We found no significant difference in either basal or insulin-stimulated glucose uptake by adipose tissue in the GLUT4^{Tg} mice compared to WT mice. The lower insulin and glucose concentration in GLUT4^{Tg} mice may in part explain the higher NEFA levels in the basal state. The higher NEFA in GLUT4^{Tg} mice may reflect long-term adaptions of the adipose tissue to the overexpression of GLUT4, or possibly to alterations in autonomic tone to the adipose tissue. However, as NEFAs were higher both in the basal and clamp states in GLUT4^{Tg} mice, greater suppression of NEFA cannot explain the improvement in MGU in response to LPS.

Improved insulin stimulated glucose disposal in GLUT4^{Tg} mice receiving LPS was not associated with a maintenance of membrane-associated glucose transport. Similar to other observations, using immunohistochemistry we observed that GLUT4^{Tg} mice had increased membrane-associated GLUT4 protein during the clamp (27, 28). However, we observed that cell surface GLUT4 was decreased by LPS in both WT and GLUT4^{Tg} mice. Inflammation is a potent inhibitor of insulin-stimulated GLUT4 translocation (29). Thus, while overexpression of GLUT4 increased total cell GLUT4 content, it could not prevent the decrease in membrane-associated GLUT4 in the setting of inflammation. It is possible that a small increase of membrane-associated transporter in GLUT4^{Tg} mice treated with LPS could have gone undetected with this method. These results were interesting in light of our previous data, which showed that insulin signaling through the PI3-K pathway was not impaired with LPS treatment (5). This pathway is believed to be the major stimulator of GLUT4 translocation to the plasma membrane under insulin-stimulated conditions. Our data are consistent with a recent report that TNF-α impairs GLUT4 translocation independent of the PI3-K pathway (30). This would suggest that other factors, besides preserving insulin-stimulated membrane associated transport activity, contributed to the improvement in MGU in GLUT4^{Tg} mice treated with LPS. As glucose-6-phosphate is a negative regulator of hexokinase, it is possible that the chronic over expression of GLUT4 lead to a compensatory upregulation of muscle glycolytic capacity that was preserved in response to LPS. We measured the content of glucose-6 phosphate in heart and skeletal muscle to determine if the content of the substrate in muscle was lower, which would reflect augmentation of downstream pathways. Both LPS-treated wild type mice and GLUT4^{Tg} mice showed a similar content of glucose-6 phosphate. Therefore, the amelioration of the deleterious effect of LPS in MGU occurring in GLUT4^{Tg} mice cannot be solely explained by upregulation of glucose transport and downstream metabolic pathways in skeletal muscle. As already mentioned, glucose conversion to lactate is increased in GLUT4^{Tg} mice. Insulin can augment muscle glycogen synthesis, glucose oxidation, and lactate release. It is possible that this adaptation of enhanced diversion of glucose to lactate was maintained in response to LPS, thus limiting the decrease in insulin–stimulated MGU. As basal MGU was also improved, it would suggest that the protection was not directly linked to improved insulin signaling. This is consistent with the lack of an alteration in insulin signaling pathway. Thus, it is likely that events outside skeletal muscle (i.e. glucose delivery) were altered to sustain MGU in response to LPS.

The GLUT4 transgene was also overexpressed in the heart, which might be cardioprotective. Improved cardiac function may have contributed to the maintenance of MGU in GLUT4^{Tg} mice treated with LPS. The dose of LPS we used impairs cardiac function and tissue perfusion as is seen in critically ill patients. These are important determinates of MGU (5). Overexpression of GLUT4 attenuated the impairment in cardiac output following LPS and improvements in insulin signaling can be cardioprotective (31). This is consistent with prior reports showing that loss of cardiac GLUT4 transport activity impairs cardiac function (32, 33), while the overexpression of glucose transporters protects both cardiac and mitochondrial function in response to stressors (34). It is unclear why overexpression of GLUT4 was protective of cardiac function. We observed that GLUT4 overexpression lowered basal cardiac *Nos2*; however, LPS augmented *Nos2* to the same extent in WT and

GLUT4^{Tg} mice, suggesting that cardiac inflammation, which can impair cardiac function, was comparable. GLUT4^{Tg} had markedly upregulated *Pdk4* expression (which would impair cardiac pyruvate oxidation), and other reports suggest overexpression of glucose transporters preserve cardiac mitochondrial function (34). As LPS impairs cardiac fat oxidation maintenance of cardiac glucose uptake may be cardioprotective (35). The sustained GLUT4 expression did not increase glucose 6 phosphate in the heart, but it may have served to protect mitochondrial function and cardiac function even though cardiac glucose oxidation was not augmented and only diversion to lactate was sustained. As MGU is very sensitive to tissue perfusion, the secondary benefit of the improved cardiac function was maintenance of MGU during inflammation. Capillary density is not increased in GLUT4^{Tg} (23). Future studies will need to be done to determine if muscle perfusion is preserved in GLUT4^{Tg} and whether this is linked to the cardiac protection in response to LPS.

Conclusion

Overexpression of muscle-specific HKII does not benefit insulin-stimulated glucose uptake in the presence of LPS, while overexpression of GLUT4 exerts a protective role. Surprisingly, this protection is not mediated solely by a preservation of membrane-associated GLUT4. Rather, preservation of cardiac function, as well as long term metabolic adaptations in muscle, limit the impairment in MGU. Thus, the endotoxin-induced impairment in both basal and insulin-stimulated MGU is driven by a complex interaction of cardiovascular and metabolic events.

Acknowledgments

This work was supported by National Institutes of Health Grants DK-078188, DK-043748 and DK-033823. OPM also received supported from DK020593 and DK059637. Special thanks to the members of the Mouse Metabolic Phenotyping Center (DK059637; Carlo Malabanan, Deanna Bracy, and Freyja James) who implanted the catheters as well as Lin Zhong who performed the echocardiography studies. We would like to thank the Vanderbilt University Hormone Assay and Analytical Core for performing insulin assays (DK059637 and DK020593). Kimberly X. Mulligan and Tammy M. Barnes were supported by the Molecular Endocrinology Training Grant T32-DK-07563.

Funding: NIH (DK-078188, DK-043748, DK-033823, DK-020593 and DK-059637).

References

1. The NICE-SUGAR Study Investigators. Intensive versus Conventional Glucose Control in Critically Ill Patients. N Engl J Med. 2009; 360:1283–97. [PubMed: 19318384]
2. van den Berghe G, Wilmer A, Hermans G, Meersseman W, Wouters PJ, Milants I, Van Wijngaerden E, Bobbaers H, Bouillon R. Intensive Insulin Therapy in the Medical ICU. N Engl J Med. 2006; 354(5):449–461. [PubMed: 16452557]
3. Elia M, De Silva A. Tight glucose control in intensive care units: an update with an emphasis on nutritional issues. Curr Opin Clin Nutr Metab Care. 2008; 11(4):465–70. [PubMed: 18542008]
4. Finfer S, Liu B, Chittock DR, Norton R, Myburgh JA, McArthur C, Mitchell I, Foster D, Dhingra V, Henderson WR, Ronco JJ, Bellomo R, Cook D, McDonald E, Dodek P, Hebert PC, Heyland DK, Robinson BG. Hypoglycemia and risk of death in critically ill patients. N Engl J Med. 2012; 367(12):1108–18. [PubMed: 22992074]
5. Mulligan KX, Morris RT, Otero YF, Wasserman DH, McGuinness OP. Disassociation of muscle insulin signaling and insulin-stimulated glucose uptake during endotoxemia. PLoS ONE. 2012; 7(1):e30160. [PubMed: 22276152]

6. Lang CH, Dobrescu C, Meszaros K. Insulin-mediated glucose uptake by individual tissues during sepsis. Metabolism. 1990; 39(10):1096–1107. [PubMed: 2215256]
7. Fan J, Li YH, Wojnar MM, Lang CH. Endotoxin-induced alterations in insulin-stimulated phosphorylation of insulin receptor, IRS-1, and MAP kinase in skeletal muscle. Shock. 1996; 6(3): 164–70. [PubMed: 8885080]
8. Fueger PT, Bracy DP, Malabanan CM, Pencek RR, Wasserman DH. Distributed control of glucose uptake by working muscles of conscious mice: roles of transport and phosphorylation. Am J Physiol Endocrinol Metab. 2004; 286(1):E77–84. [PubMed: 13129858]
9. Baron AD, Laakso M, Brechtel G, Edelman SV. Mechanism of insulin resistance in insulin-dependent diabetes mellitus: a major role for reduced skeletal muscle blood flow. J Clin Endocrinol Metab. 1991; 73(3):637–43. [PubMed: 1874938]
10. Charron MJ, Gorovits N, Laidlaw JS, Ranalletta M, Katz EB. Use of GLUT-4 null mice to study skeletal muscle glucose uptake. Clin Exp Pharmacol Physiol. 2005; 32(4):308–13. [PubMed: 15810997]
11. Lombardi AM, Moller D, Loizeau M, Girard J, Leturque A. Phenotype of transgenic mice overexpressing GLUT4 and hexokinase II in muscle. Faseb J. 1997; 11(13):1137–44. [PubMed: 9367348]
12. Braithwaite SS, Palazuk B, Colca JR, Edwards CW 3rd, Hofmann C. Reduced expression of hexokinase II in insulin-resistant diabetes. Diabetes. 1995; 44(1):43–8. [PubMed: 7813813]
13. Fueger PT. Glucose phosphorylation as a barrier to muscle glucose uptake. Clin Exp Pharmacol Physiol. 2005; 32(4):314–8. [PubMed: 15810998]
14. Olson AL, Liu ML, Moye-Rowley WS, Buse JB, Bell GI, Pessin JE. Hormonal/metabolic regulation of the human GLUT4/muscle-fat facilitative glucose transporter gene in transgenic mice. J Biol Chem. 1993; 268(13):9839–46. [PubMed: 8486663]
15. Chang PY, Jensen J, Printz RL, Granner DK, Ivy JL, Moller DE. Overexpression of hexokinase II in transgenic mice. Evidence that increased phosphorylation augments muscle glucose uptake. J Biol Chem. 1996; 271(25):14834–9. [PubMed: 8662926]
16. Ayala JE, Bracy DP, Malabanan C, James FD, Ansari T, Fueger PT, McGuinness OP, Wasserman DH. Hyperinsulinemic-euglycemic Clamps in Conscious, Unrestrained Mice. J Vis Exp. 2011; e3188
17. Lloyd B, Burrin J, Smythe P, Alberti KG. Enzymic fluorometric continuous-flow assays for blood glucose, lactate, pyruvate, alanine, glycerol, and 3-hydroxybutyrate. Clinical chemistry. 1978; 24(10):1724–9. [PubMed: 699277]
18. Zong H, Wang CC, Vaitheesvaran B, Kurland IJ, Hong W, Pessin JE. Enhanced Energy Expenditure, Glucose Utilization And Insulin Sensitivity In VAMP8 Null Mice. Diabetes. 2011; 60:30–38. [PubMed: 20876717]
19. House LM 2nd, Morris RT, Barnes TM, Lantier L, Cyphert TJ, McGuinness OP, Otero YF. Tissue inflammation and nitric oxide-mediated alterations in cardiovascular function are major determinants of endotoxin-induced insulin resistance. Cardiovasc Diabetol. 2015; 14:56. [PubMed: 25986700]
20. Tsao TS, Burcelin R, Katz EB, Huang L, Charron MJ. Enhanced insulin action due to targeted GLUT4 overexpression exclusively in muscle. Diabetes. 1996; 45(1):28–36. [PubMed: 8522056]
21. Fueger PT, Shearer J, Bracy DP, Posey KA, Pencek RR, McGuinness OP, Wasserman DH. Control of muscle glucose uptake: test of the rate-limiting step paradigm in conscious, unrestrained mice. J Physiol. 2005; 562(Pt 3):925–35. [PubMed: 15576451]
22. Deems R, Evans J, Deacon R, Honer C, Chu D, Bürki K, Fillers W, Cohen D, Young D. Expression of human GLUT4 in mice results in increased insulin action. Diabetologia. 1994; 37(11):1097–1104. [PubMed: 7867881]
23. Tsao TS, Li J, Chang KS, Stenbit AE, Galuska D, Anderson JE, Zierath JR, McCarter RJ, Charron MJ. Metabolic adaptations in skeletal muscle overexpressing GLUT4: effects on muscle and physical activity. FASEB J. 2001; 15(6):958–69. [PubMed: 11292656]
24. Ren JM, Marshall BA, Mueckler MM, McCaleb M, Amatruda JM, Shulman GI. Overexpression of Glut4 protein in muscle increases basal and insulin-stimulated whole body glucose disposal in conscious mice. J Clin Invest. 1995; 95(1):429–32. [PubMed: 7814644]

25. Lu B, Moser AH, Shigenaga JK, Feingold KR, Grunfeld C. Type II nuclear hormone receptors, coactivator, and target gene repression in adipose tissue in the acute-phase response. Journal of lipid research. 2006; 47(10):2179–90. [PubMed: 16847310]

26. Zu L, He J, Jiang H, Xu C, Pu S, Xu G. Bacterial endotoxin stimulates adipose lipolysis via toll-like receptor 4 and extracellular signal-regulated kinase pathway. J Biol Chem. 2009; 284(9): 5915–26. [PubMed: 19122198]

27. Grumbach IM, Chen W, Mertens SA, Harrison DG. A negative feedback mechanism involving nitric oxide and nuclear factor kappa-B modulates endothelial nitric oxide synthase transcription. J Mol Cell Cardiol. 2005; 39(4):595–603. [PubMed: 16099468]

28. Liang CF, Liu JT, Wang Y, Xu A, Vanhoutte PM. Toll-like receptor 4 mutation protects obese mice against endothelial dysfunction by decreasing NADPH oxidase isoforms 1 and 4. Arterioscler Thromb Vasc Biol. 2013; 33(4):777–84. [PubMed: 23413427]

29. Oliveira-Paula GH, Lacchini R, Tanus-Santos JE. Inducible nitric oxide synthase as a possible target in hypertension. Curr Drug Targets. 2014; 15(2):164–74. [PubMed: 24102471]

30. Nohara A, Okada S, Ohshima K, Pessin JE, Mori M. Cyclin-dependent kinase-5 is a key molecule in tumor necrosis factor-alpha-induced insulin resistance. The Journal of biological chemistry. 2011; 286(38):33457–65. [PubMed: 21813649]

31. Zhao P, Turdi S, Dong F, Xiao X, Su G, Zhu X, Scott GI, Ren J. Cardiac-specific overexpression of insulin-like growth factor I (IGF-1) rescues lipopolysaccharide-induced cardiac dysfunction and activation of stress signaling in murine cardiomyocytes. Shock. 2009; 32(1):100–7. [PubMed: 18948844]

32. Tian R, Abel ED. Responses of GLUT4-deficient hearts to ischemia underscore the importance of glycolysis. Circulation. 2001; 103(24):2961–6. [PubMed: 11413087]

33. Hruz PW, Yan Q, Struthers H, Jay PY. HIV protease inhibitors that block GLUT4 precipitate acute, decompensated heart failure in a mouse model of dilated cardiomyopathy. FASEB J. 2008; 22(7): 2161–7. [PubMed: 18256305]

34. Mittwede PN, Xiang L, Lu S, Clemmer JS, Hester RL. Oxidative stress contributes to orthopedic trauma-induced acute kidney injury in obese rats. Am J Physiol. 2015; 308(2):26.

35. Drosatos K, Drosatos-Tampakaki Z, Khan R, Homma S, Schulze PC, Zannis VI, Goldberg IJ. Inhibition of c-Jun-N-terminal kinase increases cardiac peroxisome proliferator-activated receptor alpha expression and fatty acid oxidation and prevents lipopolysaccharide-induced heart dysfunction. J Biol Chem. 2011; 286(42):36331–9. [PubMed: 21873422]

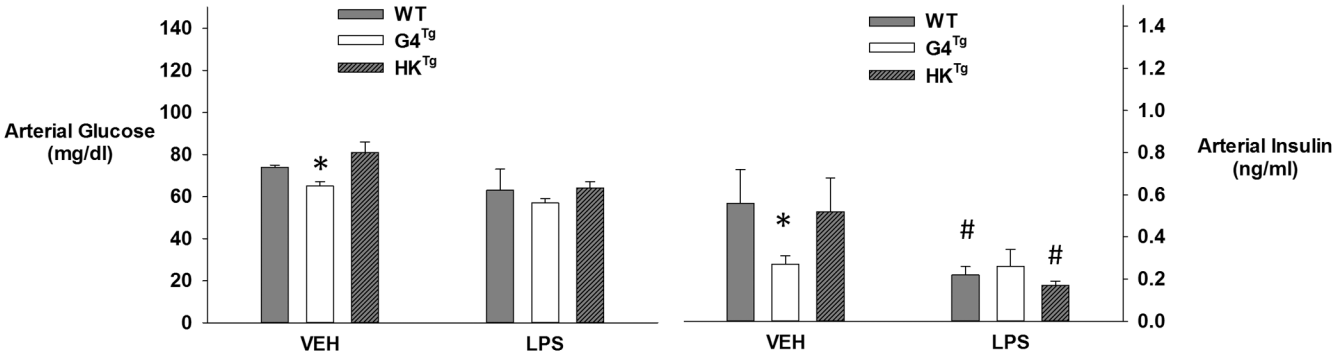

Figure 1.

Arterial blood glucose and plasma insulin levels 6 hours after vehicle (VEH) or LPS (10μg/g BW) treatment during infusion of saline in chronically catheterized conscious GLUT4 overexpressing ($G4^{Tg}$) , HKII overexpressing (HK^{Tg}) or wild-type (WT) littermate mice. Data are expressed as mean ±SEM. * indicates $p<0.05$ vs. WT, # indicates $p<0.05$ vs. VEH

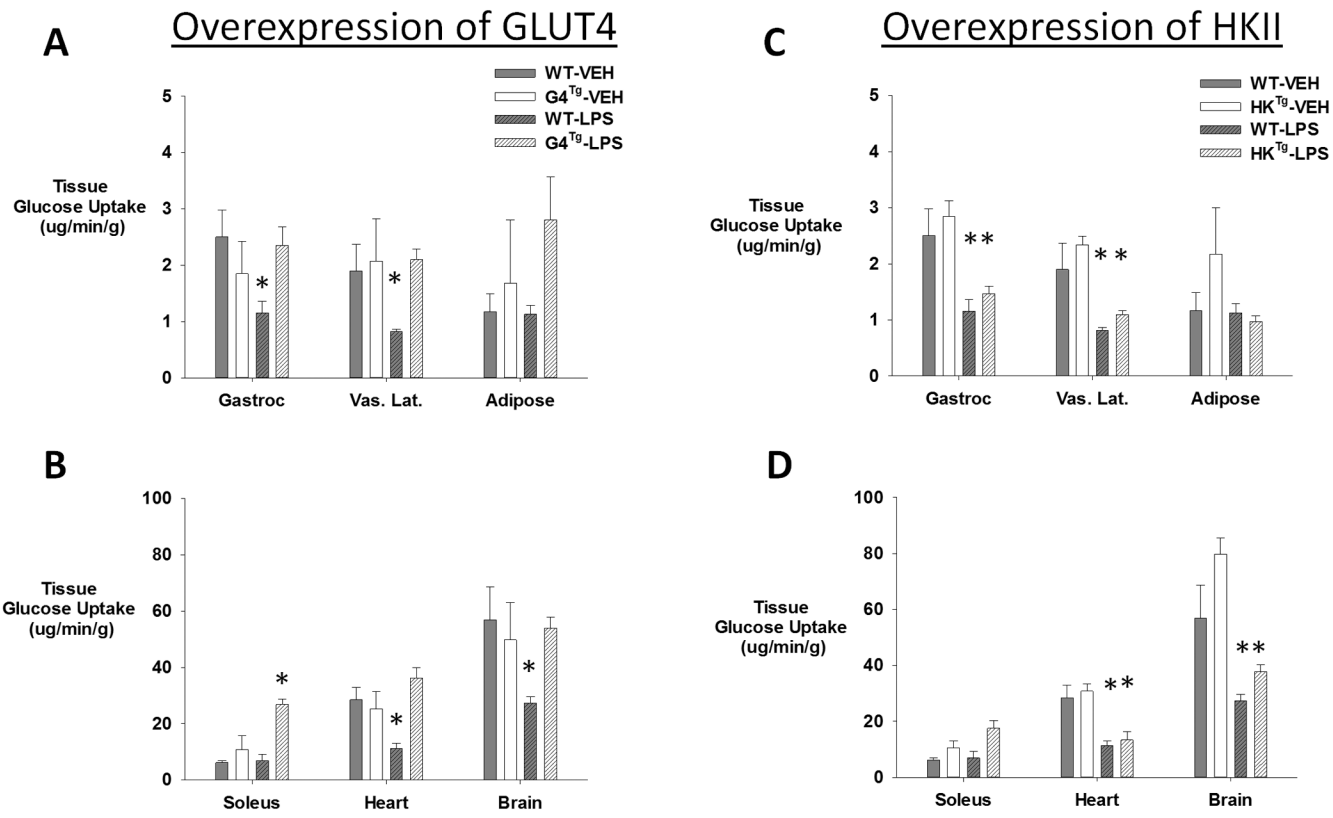

Figure 2.

A, B. Tissue glucose uptake 6 hours after vehicle (VEH) or LPS (10μg/g BW) treatment of chronically catheterized conscious GLUT4 overexpressing ($G4^{Tg}$) or wild-type (WT) littermate C57/BL6j mice during infusion of saline. Data are expressed as mean ±SEM. * indicates $p<0.05$ vs. VEH **C**, **D.** Tissue glucose uptake 6 hours after vehicle (VEH) or LPS (10μg/g BW) treatment in chronically catheterized conscious in HKII overexpressing (HK^{Tg}) or wild-type (WT) littermate C57/BL6j mice during infusion of saline. Data are expressed as mean ±SEM. * indicates $p<0.05$ vs. VEH

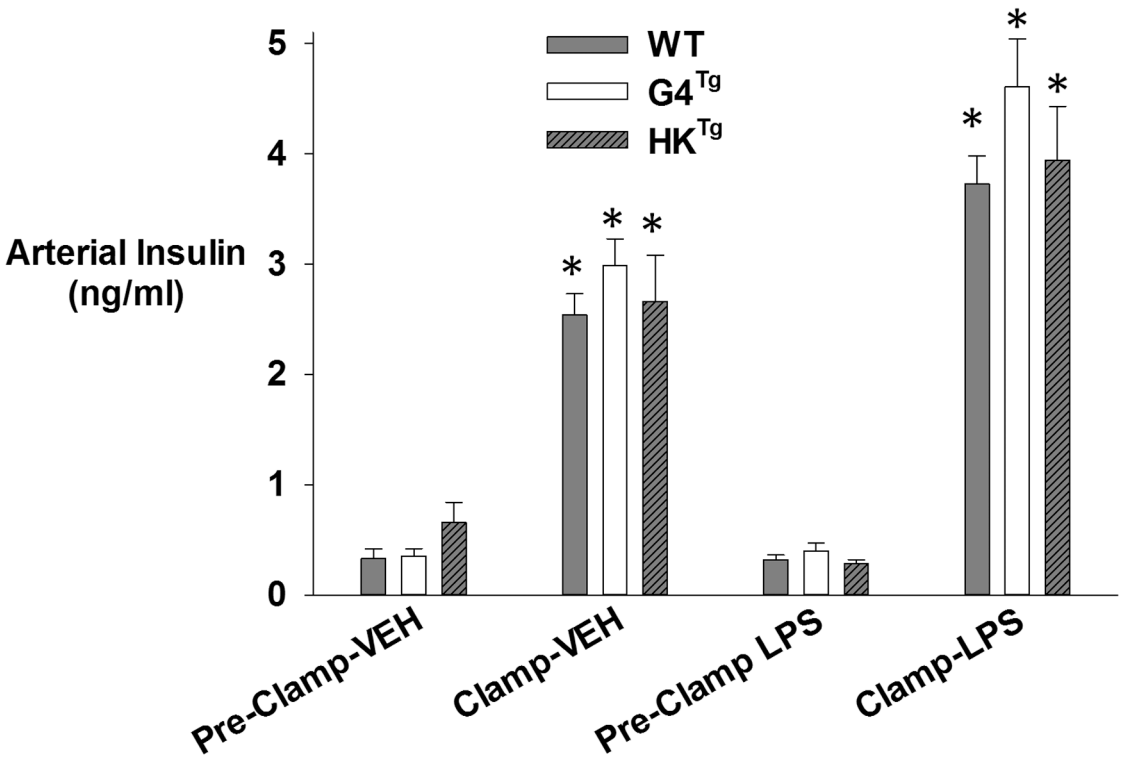

Figure 3.

Arterial plasma insulin levels in response 6 hours after treatment with vehicle (VEH) or LPS (10μg/g BW) in chronically catheterized conscious mice during the baseline period (i.e. just prior to initiation of clamp) and during a hyperinsulinemic-euglycemic clamp. Data are expressed as mean ± SEM. * (Basal vs. Clamp) $p<0.05$

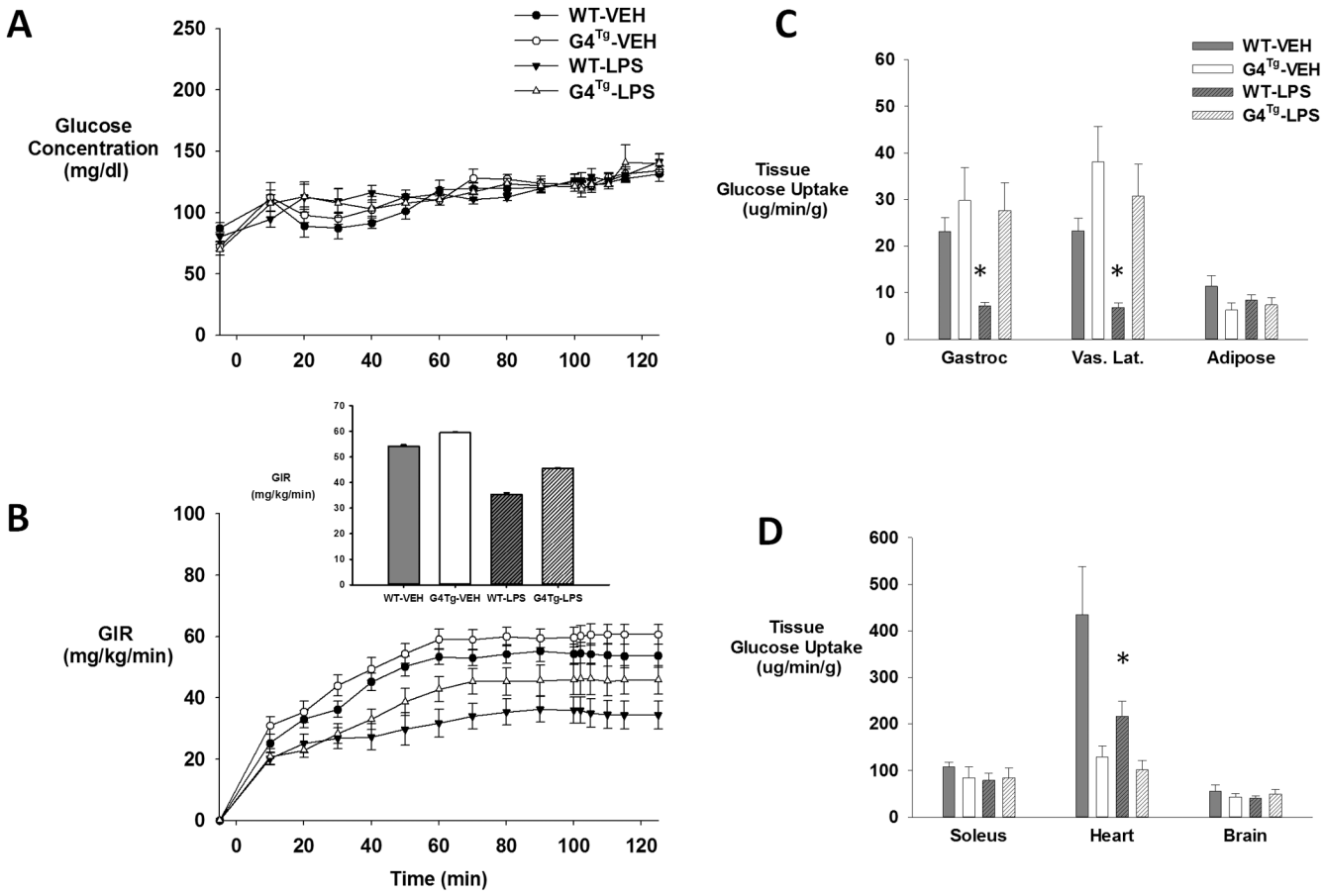

Figure 4.

Arterial blood glucose concentrations (**A**), Glucose infusion rate (GIR; inset is average GIR during last 40 min of clamp) (**B**), and tissue (gastrocnemius, *superficial vastus lateralis*, gonadal adipose tissue, soleus, heart, and brain) glucose uptake (**C**, **D**) in GLUT4^{Tg} and their wild-type littermates (WT) that received either vehicle or LPS (10μg/g BW) during a hyperinsulinemic-euglycemic clamp. Data are expressed as mean ±SEM. * (VEH vs. LPS) $p<0.05$

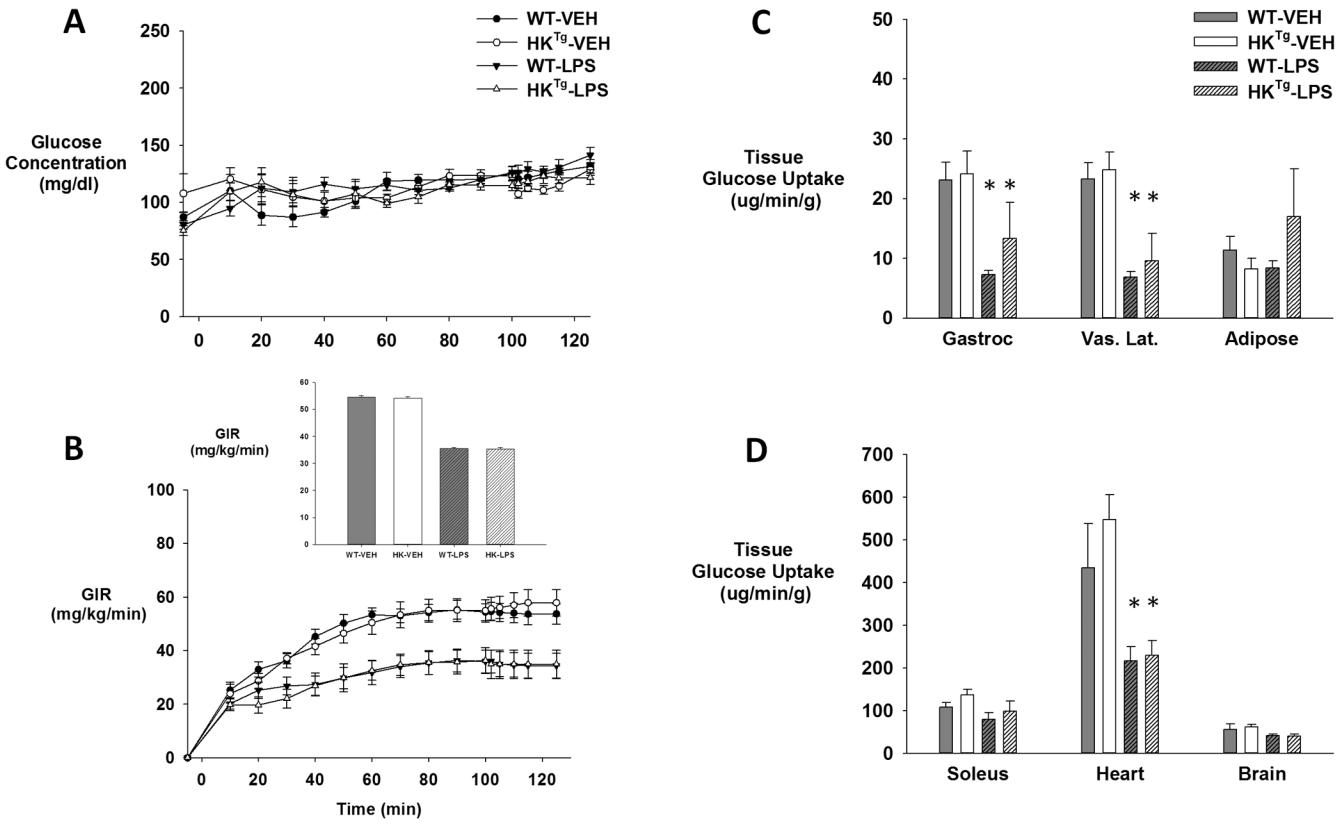

Figure 5.

Arterial blood glucose concentrations (**A**), Glucose infusion rate (GIR; inset is average GIR during last 40 min of clamp) (**B**), and tissue (*gastrocnemius, superficial vastus lateralis*, gonadal adipose tissue, soleus, heart, and brain) glucose uptake (**C,D**) in HK^{Tg} and their wild-type littermates (WT) that received either vehicle or LPS (10μg/g BW) during a hyperinsulinemic-euglycemic clamp. Data are expressed as mean ±SEM. * indicates $p<0.05$ vs. VEH

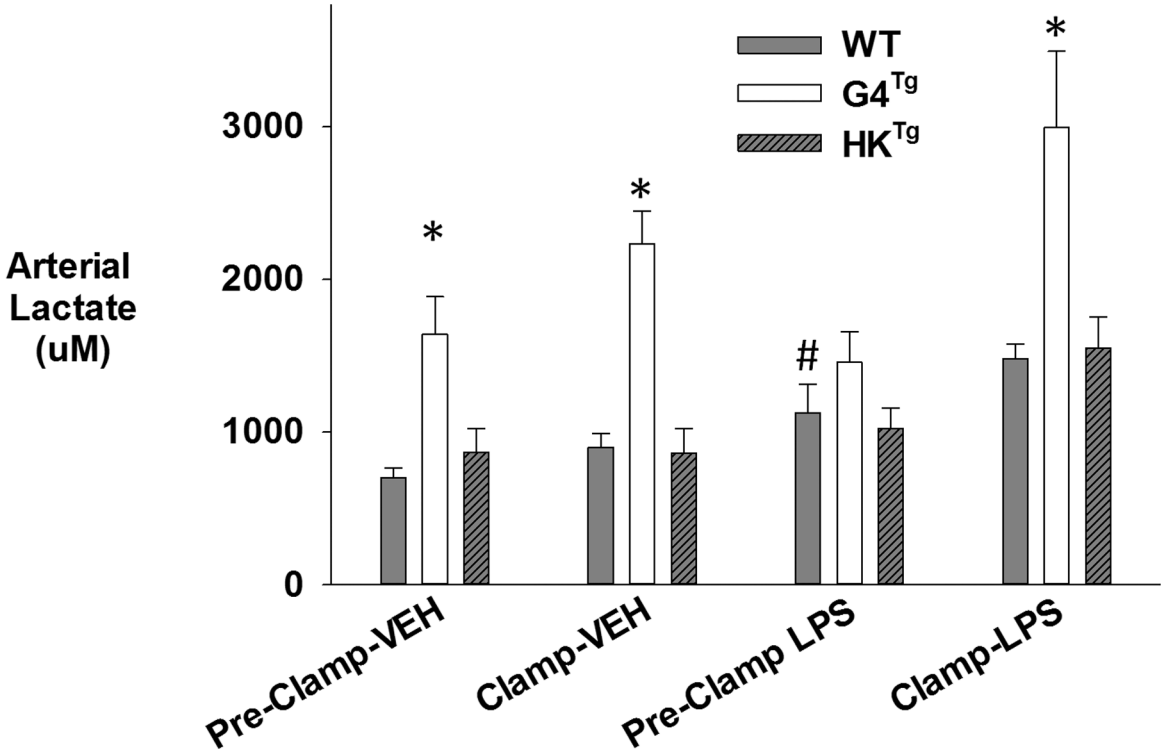

Figure 6.

Arterial plasma lactate levels (μmol/L) in response to vehicle (VEH; saline) or LPS (10μg/g BW) in chronically catheterized conscious GLUT4 overexpressing ($G4^{Tg}$) , HKII overexpressing (HK^{Tg}) or wild-type (WT) littermate mice the pre-clamp period (i.e. just prior to initiation of clamp) and after a hyperinsulinemic-euglycemic clamp. Data are expressed as mean ± SEM.* $p<0.05$ vs. WT # $p<0.05$ (VEH vs. LPS)

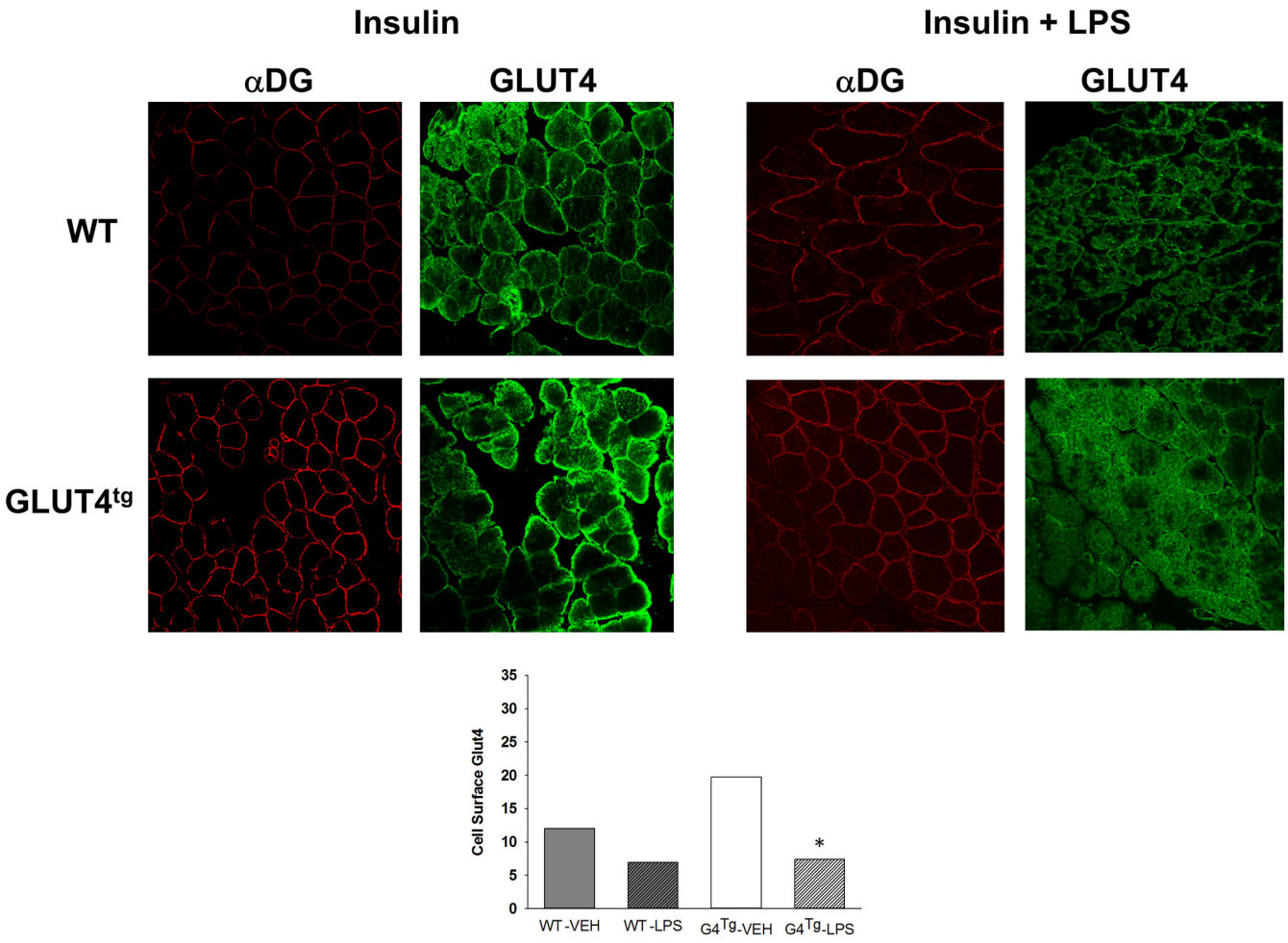

Figure 7.

Cell surface GLUT4 expression determined using confocal immunofluorescence with specific GLUT4 and the α-dystroglycan (α-DG) antibody in the gastrocnemius of WT and GLUT4 overexpressing ($GLUT4^{Tg}$) mice following VEH or LPS treatment and following a hyperinsulinemic-euglycemic clamp (Insulin=INS). Data were obtained from approximately 20 images per muscle condition from 4 independent mice for a total quantification of 80 images each. * indicates $p<0.05$ vs. VEH

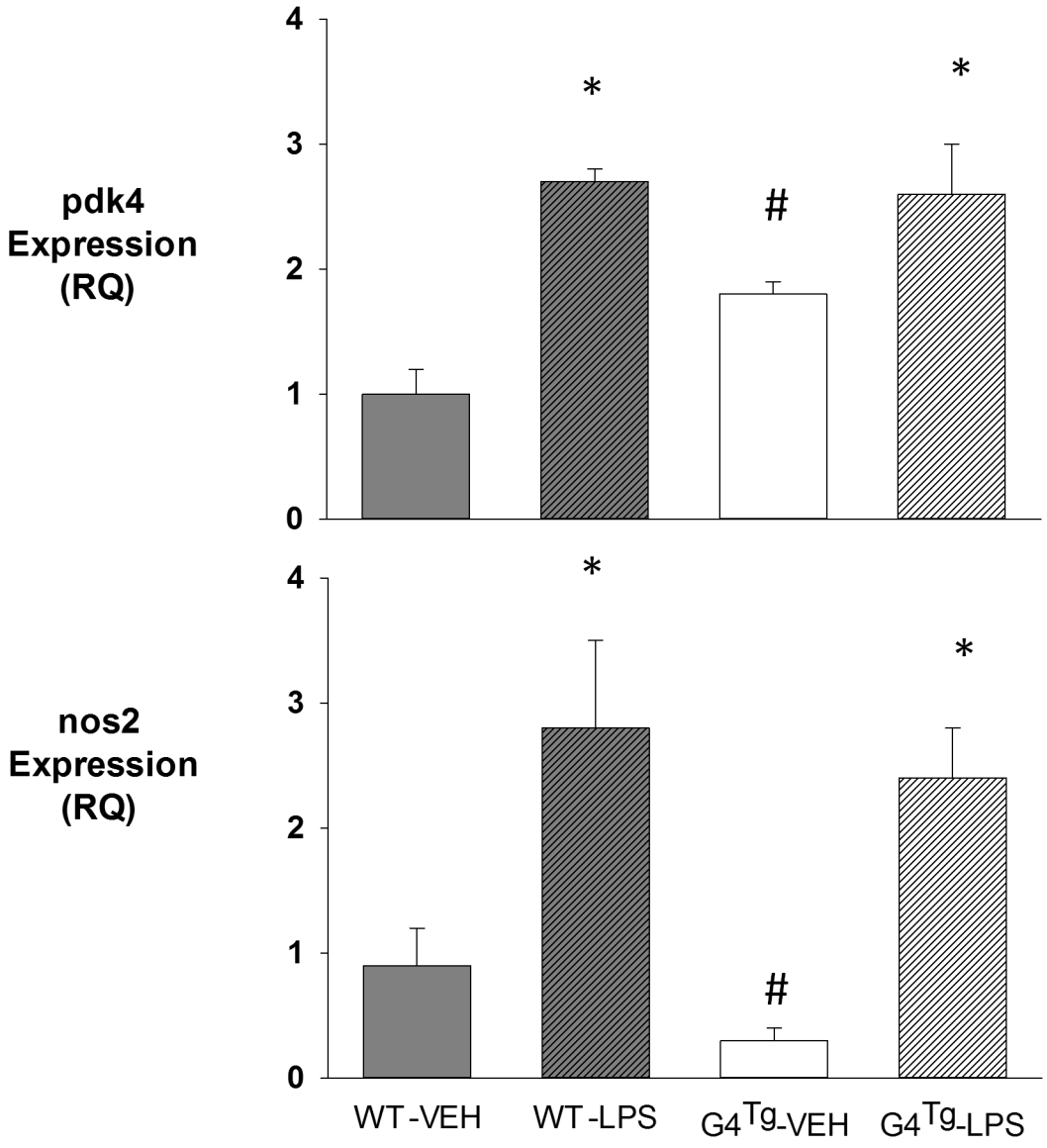

Figure 8.

Cardiac gene expression of Pdk4 (**A**) and Nos2 (**B**) in WT and GLUT4 overexpressing ($GLUT4^{Tg}$) mice, 6 hours following VEH or LPS treatment. Data are expressed as mean ±SEM. * ($G4^{Tg}$ vs. WT), # (LPS vs. VEH) $p<0.05$

Table 1

Non-esterified fatty acid levels (NEFA, μmol/mL) 6 hours after receiving vehicle (VEH) or LPS (10μg/g BW) in chronically catheterized conscious mice in the period prior to (baseline) and after initiation of a hyperinsulinemic-euglycemic clamp. Data are expressed as mean ±SEM.

	VEH		LPS	
NEFA (μmol/ml)	**Pre-Clamp**	**Clamp**	**Pre-Clamp**	**Clamp**
WT	1.71±0.11	0.56±0.17$^{\#}$	3.01±0.25	1.15±0.20$^{\#}$
GLUT4^{Tg}	3.13±0.91	1.26±0.13$^{*\#}$	5.02±0.63*	2.14±0.0.42$^{*\#}$

* p<0.05 vs. WT and

$^{\#}$ basal vs. Clamp.

Table 2

Cardiovascular parameters prior to and following VEH or LPS treatment in WT and GLUT4^{Tg} mice

Comparison of stroke volume, heart rate, and cardiac output in mice at basal (t=0) (i.e. before treatment) and 6 h after receiving vehicle (VEH) or LPS (10μg/g BW). Data are expressed as mean ± SEM.

Genotype	Basal (0 h)	6 h
Stroke Volume (μL)		
WT VEH	30.9 ± 1.2	30.6 ± 1.4
GLUT4^{Tg} VEH	37.2 ± 4.2	39.1 ± 4.2
WT LPS	33.7 ± 1.9	19.6 ± 1.1 *
GLUT4^{Tg} LPS	34.2 ± 2.7	25.8 ± 1.2
Heart Rate (bpm)		
WT Vehicle	676 ± 12	669 ± 11
GLUT4^{Tg} Vehicle	687 ± 21	588 ± 14 *
WT LPS	667 ± 10	546 ± 35 *
GLUT4^{Tg} LPS	657 ± 5	530 ± 27 *
Cardiac Output (ml/min)		
WT Vehicle	20.8 ± 0.7	20.4 ± 0.6
GLUT4^{Tg} Vehicle	25.3 ± 2.3	22.9 ± 2.5
WT LPS	22.5 ± 1.2	10.8 ± 1.1 *
GLUT4^{Tg} LPS	22.5 ± 1.8	13.6 ± 0.7

* indicates $p<0.05$ from baseline